Title
K+p INTERACTIONS NEAR 1 BeV/c

Authors
Bland, R.W.
Goldhaber, G.J
Hall, B.H.
et al.

Publication Date
1968-07-01

University of California

Ernest O. Lawrence Radiation Laboratory

K^+p INTERACTIONS NEAR 1 BeV/c

R. W. Bland, G. Goldhaber, B. H. Hall, J. A. Kadyk,
V. H. Seeger, G. H. Trilling, and C. G. Wohl

July 1968

Berkeley, California

Contribution to XIVth International
Conference on High-Energy Physics,
Vienna, August 28-September 5, 1968

UCRL-18323

UNIVERSITY OF CALIFORNIA

Lawrence Radiation Laboratory
Berkeley, California

AEC Contract No. W-7405-eng-48

K^+p INTERACTIONS NEAR 1 BeV/c

R. W. Bland, G. Goldhaber, B. H. Hall, J. A. Kadyk,
V. H. Seeger, G. H. Trilling, and C. G. Wohl

July 1968

UCRL-18323

K^+p INTERACTIONS NEAR 1 BeV/c*

R. W. Bland, G. Goldhaber, B. H. Hall, J. A. Kadyk,
V. H. Seeger, G. H. Trilling, and C. G. Wohl

Department of Physics and Lawrence Radiation Laboratory
University of California, Berkeley, California

The K^+p interaction in the momentum region just above the onset of single-pion production has been the subject of recent study. The total cross sections have been measured with considerable precision by both Cool et al.[1] and Bugg et al.[2] and the results of these experiments are shown in Fig. 1. Perhaps the most interesting feature is the structure in the neighborhood of 1.25 BeV/c. In addition the data of Cool et al. show wiggles in the total cross section at ~ 1.7 and ~ 2.7 BeV/c, of much smaller amplitude than the large peak at 1.25 BeV/c.

Detailed study of elastic and inelastic processes in the general vicinity of this structure has been carried out in an analysis of film obtained in an exposure of the LRL 25-inch bubble chamber to a separated K^+ beam at several momenta between 0.860 and 1.58 BeV/c. Results on certain aspects of this analysis have already been published.[3] In the present paper we emphasize particularly those features which have not received detailed discussion. We divide our consideration into three parts: (1) the behavior of the elastic and inelastic cross sections, (2) details of the elastic scattering, and (3) the inelastic processes.

1. Behavior of Elastic and Inelastic Cross Sections

In Fig. 2 we show the cross sections for the processes:

$$K^+ + p \rightarrow K^+ + p \quad (1)$$

$$K^+ + p \rightarrow K + N + \pi \quad (2)$$

$$K^+ + p \rightarrow K + N + \pi + \pi \quad (3)$$

over the momentum region between 0.86 and 3.5 BeV/c. The experimental data used in the figure include results of other experiments.[4] Two explanatory remarks on the way these data are compiled are in order:

(i) The accurate counter data[1,2] on total cross sections are used to renormalize cross sections whenever the contributions of all channels are available.

(ii) Only three of the five $KN\pi\pi$ final states are accessible to kinematic fitting, namely $K^+p\pi^+\pi^-$, $K^0p\pi^+\pi^0$, and $K^0n\pi^+\pi^+$. The other two channels, $K^+p\pi^0\pi^0$ and $K^+n\pi^+\pi^0$, involve two unseen neutrals. To obtain a total $KN\pi\pi$ cross section we have assumed that the $KN\pi\pi$ final states are dominated by K^*N^* production, a supposition which has good experimental support even down to 1.58 BeV/c, near the threshold for K^*N^*. On this assumption the unseen final states represent 8% of the total $KN\pi\pi$ production and the correction is small.

The curves in Fig. 2 are smooth, hand-drawn representations of the data. The general behavior of the elastic and inelastic final states can be summarized as follows:

(a) The elastic scattering cross section drops steadily from about 12 mb at 800 MeV/c to 4.4 mb at 3.5 BeV/c. This behavior is readily interpretable in terms of a Regge exchange formulation in that while the Pomeranchuk contribution remains constant, the contributions of the lower lying trajectories (ρ, ω, A_2, P', etc.) are dropping as the K momentum increases. One may question the applicability of a Regge model at the low momenta under study, but as will be continually emphasized in this discussion, the K^+p system appears to become nearly "asymptotic" in its behavior at momenta as low as 1.2 BeV/c. More detailed discussion of this point will be given further on.

(b) The single-pion-production channels dominate the inelastic processes up to 1.5 BeV/c. They rise rapidly as the K^+ momentum increases above 0.8 BeV/c, reach a broad maximum of about 8 mb near 1.45 BeV/c, and then slowly and smoothly drop off.

(c) The two-pion production remains very small from threshold (0.81 BeV/c) to about 1.5 BeV/c, and then rises abruptly. Presumably the explanation of this behavior lies in the dominance of K^*N^* production, whose effective threshold lies near 1.6 BeV/c.

(d) Three-pion production (not shown in Fig. 2) is negligible up to 2 BeV/c.

When the smooth curves given in Fig. 2 are added together, they produce the total cross-section curve shown in Fig. 1. The remarkable feature is that the structure at 1.25 BeV/c is very well reconstructed by the sum of three structureless channel cross sections. The interpretation of that structure in terms of contributions from the various channels can then be expressed in the following terms: The rise above 0.8 BeV/c is associated with the rapidly rising single-pion cross section, the maximum being reached when this rate of rise is just balanced by the rate of drop of the elastic cross section. This maximum is followed by a drop as the single-pion cross section levels off. Finally, this drop is arrested when the two-pion cross section begins to rise at about 1.5 BeV/c. Thus the structure in the total cross section at 1.25 BeV/c does not arise from structure in any single partial cross section. Rather it is a consequence of the sharp rises of the single- and double-pion-production channels at widely separated thresholds. Although the available data are not sufficient to prove it, it is quite reasonable to suppose that the additional small structure observed by Cool et al. may be a consequence of the fact that the 3π cross section does not become significant until K momenta substantially above 2 BeV/c, at which point the 2π channel has ceased rising and the combined KN, $KN\pi$, and $KN\pi\pi$ cross sections are rapidly dropping.

It should be emphasized that this interpretation of the structure in the total cross section is at variance with a conventional resonance interpretation but completely in accordance with the fact that the detailed behavior of angular distributions and polarizations in the inelastic channels appears to be smooth even through the momentum region in which the structure in the total cross section occurs.

2. Elastic Scattering

Angular distributions for elastic scattering obtained in this experiment are shown in Fig. 3. Also shown is the differential cross section at 0.78 BeV/c reported by Focardi et al.[5] The general features can be summarized as follows: The S wave behavior characteristic up to 0.7 BeV/c is modified principally by the presence of a $\cos^2\theta$ term quite apparent in the distributions at 0.78, 0.86 and 0.96 BeV/c. As pointed out in Focardi et al. this feature is most easily interpreted by the presence of significant D wave amplitudes, the DS interference producing the $\cos^2\theta$ behavior. At 1.2 BeV/c, and above, a well-defined diffraction peak is produced by virtue of the fact that inelastic processes produce strong P-wave absorption (as is known from detailed studies of the inelastic processes), and the nearly imaginary P amplitudes interfere strongly with the dominant repulsive S wave to produce the large forward-backward asymmetry.

We have attempted to make a phase shift analysis at the momenta below 1.2 BeV/c where the absorption by inelastic channels does not appear to be very large. At 1.2 BeV/c and higher momenta the results of such an analysis are of course quite sensitive to assumptions about the partial wave distribution of the inelastic processes, which is very difficult to determine with any precision. We have restricted ourselves to the dominant repulsive S wave solution, type A^-, which as shown by S. Goldhaber et al.[6] is the only one that agrees with the Coulomb interference and momentum dependence observed below 640 MeV/c. In order to further restrict somewhat the range of possible solutions we have applied continuity conditions to force smoothness from one momentum to the next. More precisely, data from three momenta were handled simultaneously, the program being to minimize a function equal to $\chi^2 + C \sum_{\text{waves}} [(\delta_1 - \delta_2)^2 + (\delta_2 - \delta_3)^2]$ where the subscripts 1, 2, and 3 refer to the momenta used and C is a constant. The value of C was adjusted to be as large as possible and still be compatible with the condition that the χ^2 corresponding to the above minimization does not differ by more than ~ 0.5 from the minimum χ^2 reached when the constant C is set equal to zero (that is, when each momentum is fitted individually). The effect of this procedure is to choose that location in the large χ^2 valley for each momentum which matches best a corresponding location for an adjacent momentum. The absorption parameters η for each of the momenta were estimated from information derived in the study of the inelastic processes.[3] Specifically, at 0.86 and 0.96 BeV/c an analysis of the $K^o p \pi^+$ final state provided estimates of how much of the incident $P_{1/2}$ and $P_{3/2}$ waves go into KN^* production (other waves playing little role in this process at these energies). The remaining inelastic cross section was assumed to come from a three-body background in which all particle pairs are in relative S states; such a background is fed by an incident $P_{1/2}$ wave. The absorption parameters used at 0.78 BeV/c were extrapolated from those at 0.86 and 0.96 BeV/c. Our procedures thus differ markedly from the phase shift analysis of Lea et al.[7] It may be noted that the inelastic amplitudes which we find to be dominant, namely the $P_{1/2}$ and $P_{3/2}$ waves, are not a combination from which Lea et al. find a good fit. Table I gives the phase shifts obtained in a simultaneous fit at 0.78, 0.86 and 0.96 BeV/c.[8] The absorption parameters assumed are also given in Table I. These solutions are exhibited in the Argand diagram in Fig. 4. The two solutions are related by a Yang-Fermi transformation and can in principle be distinguished by a polarization measurement. The fits given by either of these solutions are shown by the curves in Fig. 3. The predicted polarizations[9] for the two solutions are given in Fig. 5. A measurement at 780 MeV/c by Femino et al.[10] favors Solution I, but more precise polarization data will be required for a conclusive choice between the two solutions. For either solution the $S_{1/2}$ amplitude remains the dominant one up to at least 0.96 BeV/c, whereas the P and D amplitudes remain small.

We now consider the higher momentum elastic scattering data. As indicated above the results of phase-shift analyses are sensitive to the absorption parameters η which are not well known. Nevertheless we have made a simultaneous fit of data at 0.86, 0.96 and 1.2 BeV/c. In this case we have not fed in a priori absorption parameters for the S and P waves at 1.2 BeV/c but have let them be determined as well by the fit. The results are that there appears to be little or no absorption in the S wave and large absorption in the $P_{1/2}$ and $P_{3/2}$ waves, although the relative contributions of the $P_{1/2}$ and $P_{3/2}$ states are not well determined by the data. The S-wave phase shift remains essentially unchanged. The D-wave phase shifts are of course not well determined but it is possible to get good fits without requiring any significant change from the values at the lower momenta.

It is interesting to note the variation of $d\sigma/d\Omega\ (180^{\circ})$ with momentum, shown in Fig. 6. Below 900 MeV/c the predominantly positive P-wave phase shifts combine with the large negative S-wave phase shift to produce an asymmetry which favors the backward direction. As the momentum increases the rapidly rising N^* production leads to large P-wave inelasticity with the consequence that the P-wave elastic amplitude changes from being small, nearly real, and positive to large, and imaginary, reversing the sign of the asymmetry. Thus the maximum in $d\sigma/d\Omega\ (180^{\circ})$ near 860 MeV/c has a straightforward interpretation in terms of readily understood variations of the amplitudes.

We now consider a representation of the data at and above 1.2 BeV/c in terms of its diffractive behavior. Figure 7 shows a representation of elastic data including our measurements at 1.2 and 1.36 BeV/c, those of Bettini et al.[4b] at 1.45 BeV/c, and those of S. Goldhaber et al.[4c] at 1.96 BeV/c, in terms of momentum transfer on a semilog scale. It is apparent that up to $-t = 0.8\ (\mathrm{BeV/c})^2$ the data can be represented by a straight line whose intercept at $t = 0$ is $\sim 20\ \mathrm{mb/(BeV/c)^2}$ and whose slope becomes steeper as the momentum increases. Table II gives values of slopes and intercepts between 1.2 and 1.96 BeV/c. It may be noted that this description applies correctly to K^+p elastic scattering up to 14.8 BeV/c, at which point the intercept is still about 20 $\mathrm{mb/(BeV/c)^2}$ but the slope has steepened by a factor of about 2.3 from its value at 1.2 BeV/c.[11] In view of this correspondence with the high energy behavior we have compared the data with a modified version of the Regge pole fit of Rarita and Phillips.[12] The modification consists of replacing the contributions of the ρ and A_2 trajectories in the fits of Rarita and Phillips by more appropriate ones based on the charge-exchange fit of Rarita and Schwarzschild.[13] It has been checked that this change has no significant effect on the high energy fits, but does produce some modifications at the low energies. The calculated curves based on the Regge fit are shown in Fig. 7. The agreement is remarkably good considering that the lowest momentum used to determine the parameters of the fit is 6.8 BeV/c. The main discrepancy is that for their parameters the experimental shrinkage of the diffraction peak between 1.2 and 14.8 BeV/c is about 20% larger than that given by the Regge fit.

3. Inelastic Processes

Inelastic processes have already been discussed in some detail and there is not a great deal of new information to add. The cross sections for KN^* and NK^* production are given in Fig. 8. It should be noted that the structure which appeared in the KN^* cross section in Ref. 3 resulted from a preliminary fit with smaller statistics at 1.36 BeV/c, and is not present in the curve of Fig. 8 which is completely smooth. As discussed in the beginning of this paper we associate the structure in the Cool peak as arising from the superposition of individual smooth channel cross sections and not as arising from structure in a single channel like KN^*.

The smoothness of the behavior of the KN^* channel is further emphasized by Fig. 9 and 10 which show the N^* and K^* density matrix elements as a function of momentum over a wide range of momenta.[14] It is clear from these figures that, as with the elastic scattering, asymptotic behavior is practically reached at 1.2 BeV/c.

In conclusion, we have seen that all properties of the individual channels--cross sections, angular distributions, and polarizations--vary smoothly with energy, rapidly approaching the asymptotic high-energy behavior. These features strongly reinforce the argument made in the discussion concerning cross sections that the behavior of individual channels is very smooth and exhibits no structure as a function of momentum. This argues very strongly <u>against</u> any conventional resonance interpretation of the structure in the total cross section.

We wish to acknowledge the important contributions of M. Bowler, J. L. Brown, and S. Goldhaber to the early phases of this experiment, as well as the help of C. Fu and H. Tanz in preparing this paper.

REFERENCES

*Work supported by the U. S. Atomic Energy Commission.

1. R. L. Cool, G. Giacomelli, T. F. Kycia, B. A. Leontić, K. K. Li, A. Lundby, and J. Teiger, Phys. Rev. Letters 17, 102 (1966). The values of σ_t used in Fig. 1 differ slightly from those given in this reference and were supplied by T. Kycia.

2. D. V. Bugg, R. S. Gilmore, K. M. Knight, D. C. Salter, G. H. Stafford, E. J. N. Wilson, J. D. Davies, J. D. Dowell, P. M. Hattersley, R. J. Homer, A. W. O'Dell, A. A. Carter, R. J. Tapper, and K. F. Riley, Phys. Rev. 168, 1466 (1968).

3. R. W. Bland, M. G. Bowler, J. L. Brown, G. Goldhaber, S. Goldhaber, V. H. Seeger, and G. H. Trilling, Phys. Rev. Letters 18, 1077 (1967).

4. a) 810 MeV/c K^+p elastic scattering--T. F. Stubbs, H. Bradner, W. Chinowsky, G. Goldhaber, S. Goldhaber, W. Slater, D. M. Stork, and H. K. Ticho, Phys. Rev. Letters 7, 188 (1961); 810 MeV/c $K^+p \rightarrow K\pi N$--J. Fisk, H. K. Ticho, D. H. Stork, W. Chinowsky, G. Goldhaber, S. Goldhaber, and T. F. Stubbs, Proceedings of the 1962 International Conference on High-Energy Physics at CERN, J. Prentki, editor (CERN, Geneva 23, Switzerland).

   b) 1450 MeV/c--A. Bettini, M. Cresti, S. Limentani, L. Perruzzo, R. Santangelo, D. Locke, D. J. Crennell, W. T. Davies, and P. B. Jones, Physics Letters 16, 83 (1965); G. B. Chadwick, D. J. Crennell, W. T. Davies, M. Derrick, J. H. Mulvey, P. B. Jones, D. Radojicic, C. A. Wilkinson, A. Bettini, M. Cresti, S. Limentani, L. Perruzzo, and R. Santangelo, Physics Letters 6, 309 (1963).

   c) 1960 MeV/c--W. Chinowsky, G. Goldhaber, S. Goldhaber, T. O'Halloran, and B. Schwarzschild, Phys. Rev. 139B, 1411 (1965).

d) 2650 MeV/c--R. Newman, W. Chinowsky, J. Schultz, W. B. Johnson, and R. R. Larsen, Phys. Rev. 158, 1310 (1967).

e) 2970 MeV/c--M. Ferro-Luzzi, R. George, Y. Goldschmidt-Clermont, V. P. Henri, B. Jongejans, D. W. G. Leith, G. R. Lynch, F. Muller, and J.-M. Perreau, Nuovo Cimento 36, 1101 (1965) and 39, 417 (1965); J. Debaisieux, F. Grard, J. Heüghebaert, L. Pape, R. Windmolders, R. George, Y. Goldschmidt-Clermont, V. P. Henri, D. W. G. Leith, G. R. Lynch, F. Muller, J.-M. Perreau, G. Otter, and P. Sällström, Nuovo Cimento 43A, 142 (1966); P. Sällström, G. Otter, and G. Ekspong, Nuovo Cimento 49A, 348 (1967).

f) 3460 MeV/c--R. George, Y. Goldschmidt-Clermont, V. P. Henri, B. Jongejans, M. Krammer, F. Muller, J.-M. Perreau, W. De Baere, J. Debaisieux, P. Dufour, F. Grard, J. Heüghebaert, L. Pape, P. Peeters, F. Verbeure, and R. Windmolders, Nuovo Cimento 49A, 9 (1967); W. De Baere, J. Debaisieux, P. Dufour, F. Grard, J. Heüghebaert, L. Pape, P. Peeters, F. Verbeure, R. Windmolders, R. George, Y. Goldschmidt-Clermont, V. P. Henri, B. Jongejans, D. W. G. Leith, A. Moisseev, F. Muller, J.-M. Perreau, V. Yarba, Nuovo Cimento 45A, 885 (1966); W. De Baere, J. Debaisieux, P. Dufour, F. Grard, J. Heüghebaert, L. Pape, P. Peeters, F. Verbeure, R. Windmolders, Y. Goldschmidt-Clermont, V. P. Henri, B. Jongejans, A. Moisseev, F. Muller, J.-M. Perreau, A. Prokeš, and V. Yarba, Nuovo Cimento 51A, 401 (1967).

5. 785 MeV/c K^+p elastic scattering--S. Focardi, A. Minguzzi-Ranzi, L. Monari, G. Saltini, P. Serra, T. A. Filippas, and V. P. Henri, Physics Letters 24B, 314 (1967).

6. S. Goldhaber, W. Chinowsky, G. Goldhaber, W. Lee, T. O'Halloran, T. F. Stubbs, B. M. Pjerrou, D. H. Stork, and H. K. Ticho, Phys. Rev. Letters 9, 135 (1962).

7. A. T. Lea, B. R. Martin, and G. C. Oades, Phys. Rev. 165, 1770 (1968).

8. An additional solution to the joint fit, A_{II}^{-}, was found having a corresponding single-energy χ^2 minimum only at 960 MeV/c. The single-energy solution is: $\delta_{S_{1/2}} = -50\pm1.2$, $\delta_{P_{1/2}} = 0.7\pm3.7$, $\delta_{P_{3/2}} = 3.2\pm2.6$, $\delta_{D_{3/2}} = -4.7\pm1.7$, $\delta_{D_{5/2}} = 0.9\pm1.7$, with the values of η given in Table I.

9. We have defined the polarization with respect to the normal $\hat{n} = \frac{\hat{q} \times \hat{p}}{|\hat{q} \times \hat{p}|}$ where $\hat{q}$ and $\hat{p}$ are unit vectors along the incoming K and the outgoing proton respectively.

10. S. Femino, S. Jannelli, F. Mezzanares, L. Monari, and P. Serra, Nuovo Cimento 50A, 371 (1967).

11. K. J. Foley, S. J. Lindenbaum, W. A. Love, S. Ozaki, J. J. Russell, and L. C. L. Yuan, Phys. Rev. Letters 11, 503 (1963).

12. R. J. N. Phillips and W. Rarita, Phys. Rev. 139, B1336 (1965).

13. W. Rarita and B. M. Schwarzschild, Phys. Rev. 162, 1378 (1967).

14. a) 0.865-1.36 BeV/c--R. Bland, Ph.D. Thesis, University of California (1968).

b) 1.58 BeV/c--M. G. Bowler, R. W. Bland, J. L. Brown, G. Goldhaber, J. A. Kadyk, V. Seeger, and G. H. Trilling, Lawrence Radiation Laboratory Report UCRL-16370 (1965), unpublished; R. W. Bland, M. G. Bowler, J. L. Brown, G. Goldhaber, S. Goldhaber, J. A. Kadyk, V. Seeger, and G. H. Trilling, Report submitted to the XIIIth International Conference on High-Energy Physics, Berkeley, California, August 31 to September 7, 1966.

c) 1.96 GeV/c--S. Goldhaber, W. Chinowsky, G. Goldhaber, and T. O'Halloran, Phys. Rev. 142, 913 (1966).

d) 2.26 BeV/c--F. Bomse, S. Borenstein, J. Cole, D. Gillespie, R. Kraemer, G. Luste, I. Miller, E. Moses, A. Pevsner, R. Singh, and R. Zdanis, Phys. Rev. 158, 1298 (1967).

e) 2.65 BeV/c--R. Newman, W. Chinowsky, J. Schultz, W. B. Johnson, and R. K. Larsen, Phys. Rev. 158, 1310 (1967).

f) 2.965 BeV/c--G. R. Lynch, M. Ferro-Luzzi, R. George, Y. Goldschmidt-Clermont, V. P. Henri, B. Jongejans, D. W. G. Leith, F. Muller, and J.-M. Perreau, Physics Letters 9, 359 (1964).

g) 2.970 BeV/c--P. Sällström and G. Blomqvist, Arkiv för Fysik 37, 463 (1968).

h) 3.460 BeV/c--W. De Baere, J. Debaisieux, P. Dufour, F. Grard, J. Heughebaert, L. Pape, P. Peeters, F. Verbeure, R. Windmolders, Y. Goldschmidt-Clermont, V. P. Henri, B. Jongejans, A. Moisseev, F. Muller, J.-M. Perreau, A. Prokeš, and V. Yarba, CERN preprint No. CERN/D.Ph.II/PHYSICS 67-5 (1967), to be submitted to Nuovo Cimento.

i) 4.6 BeV/c--C. Fu, G. Goldhaber, B. Shen, Lawrence Radiation Laboratory (unpublished).

j) Unpublished data from the authors of Ref. 14h as quoted in J. D. Jackson, J. T. Donahue, K. Gottfried, R. Keyser, and B. E. Y. Svennson, Phys. Rev. 139, B428 (1965).

k) 10 GeV/c--Birmingham-Glasgow-Oxford Collaboration.

Table I. Phase shifts for fit at 0.78, 0.86, and 0.96 BeV/c.

		A_I^- solution			A_{III}^- solution		
Momentum (BeV/c)		0.78	0.86	0.96	0.78	0.86	0.96
$S_{1/2}$	η	1.0	1.0	1.0	1.0	1.0	1.0
	δ	-39 ± 3.5	-42 ± 8.7	-45 ± 5.2	-39 ± 3.5	-43 ± 8.6	-45 ± 5.3
$P_{1/2}$	η	0.967	0.913	0.792	0.967	0.913	0.792
	δ	-11 ± 7.8	-11 ± 8.6	-13 ± 7.8	14 ± 8.8	17 ± 10.4	20 ± 9.1
$P_{3/2}$	η	0.996	0.975	0.920	0.996	0.975	0.920
	δ	7 ± 4.4	11 ± 4.5	10 ± 4.1	-5 ± 1.9	-2.3 ± 2.7	-3.6 ± 2.5
$D_{3/2}$	η	1.0	0.998	0.993	1.0	0.998	0.993
	δ	-0.4 ± 2.3	-1.8 ± 0.7	-1.8 ± 0.8	-2.7 ± 1.3	-1.7 ± 1.8	-2.5 ± 1.3
$D_{5/2}$	η	1.0	0.998	0.988	1.0	0.998	0.988
	δ	-2.3 ± 0.7	-2.3 ± 1.5	-2.3 ± 0.9	-0.8 ± 1.7	-2.8 ± 0.6	-1.8 ± 0.6

Table II. Parameters for exponential fits to K^+p elastic scattering, $\frac{d\sigma}{dt} = \alpha\, e^{\beta t}$.

K momentum (BeV/c)	$\alpha = \frac{d\sigma}{dt}(t=0)$ [mb/(BeV/c)^2]	β (BeV/c)$^{-2}$
1.2	22.2±1.0	2.34±0.10
1.36	23.4±1.7	2.51±0.15
1.45	23.3±1.4	2.62±0.11
1.96	20.0±2.3	3.02±0.15

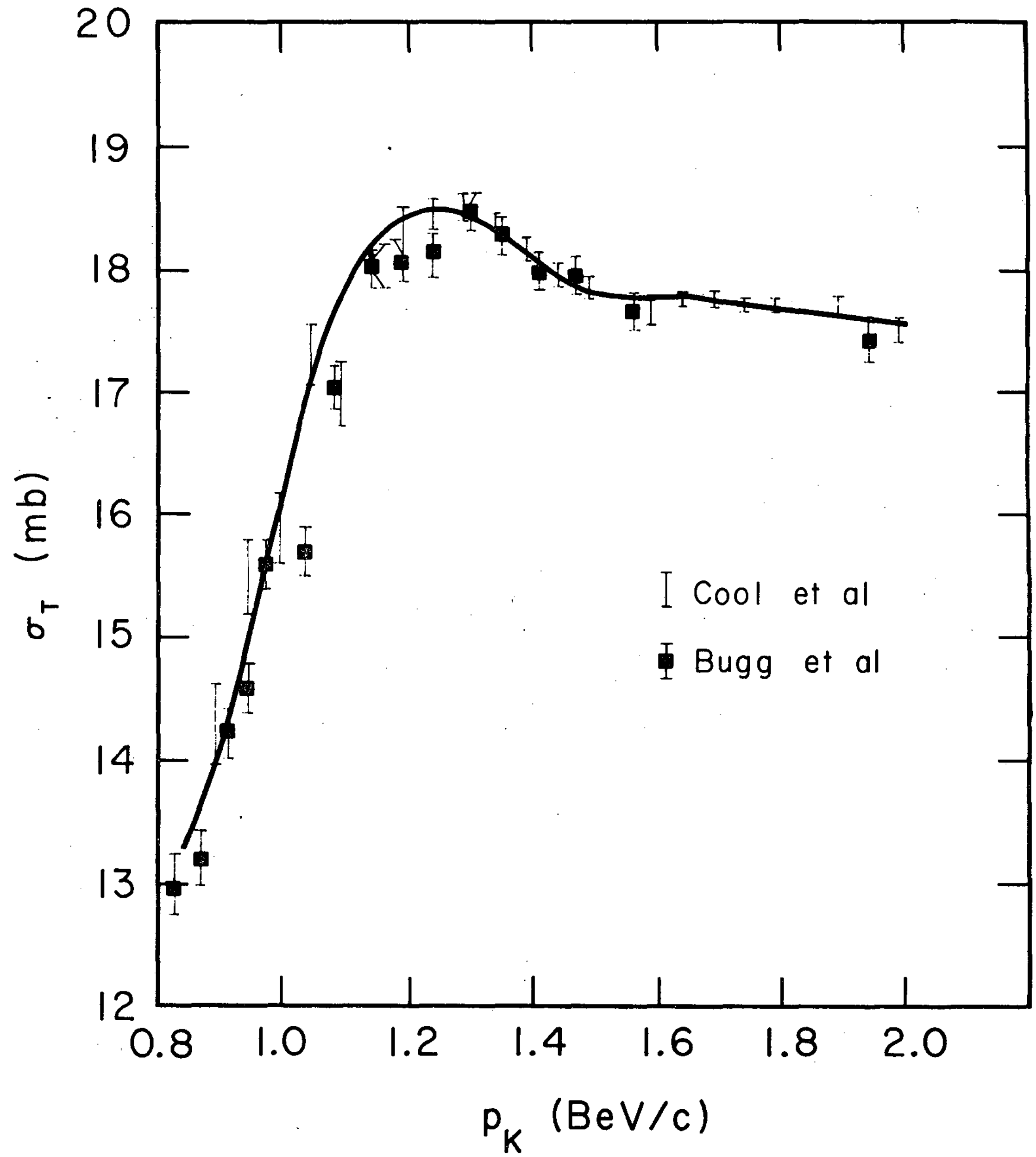

Fig. 1. Total K^+p cross section: the data points are from Cool et al. and Bugg et al., and the solid curve is sum of curves show in Fig. 2.

XBL 688-3483

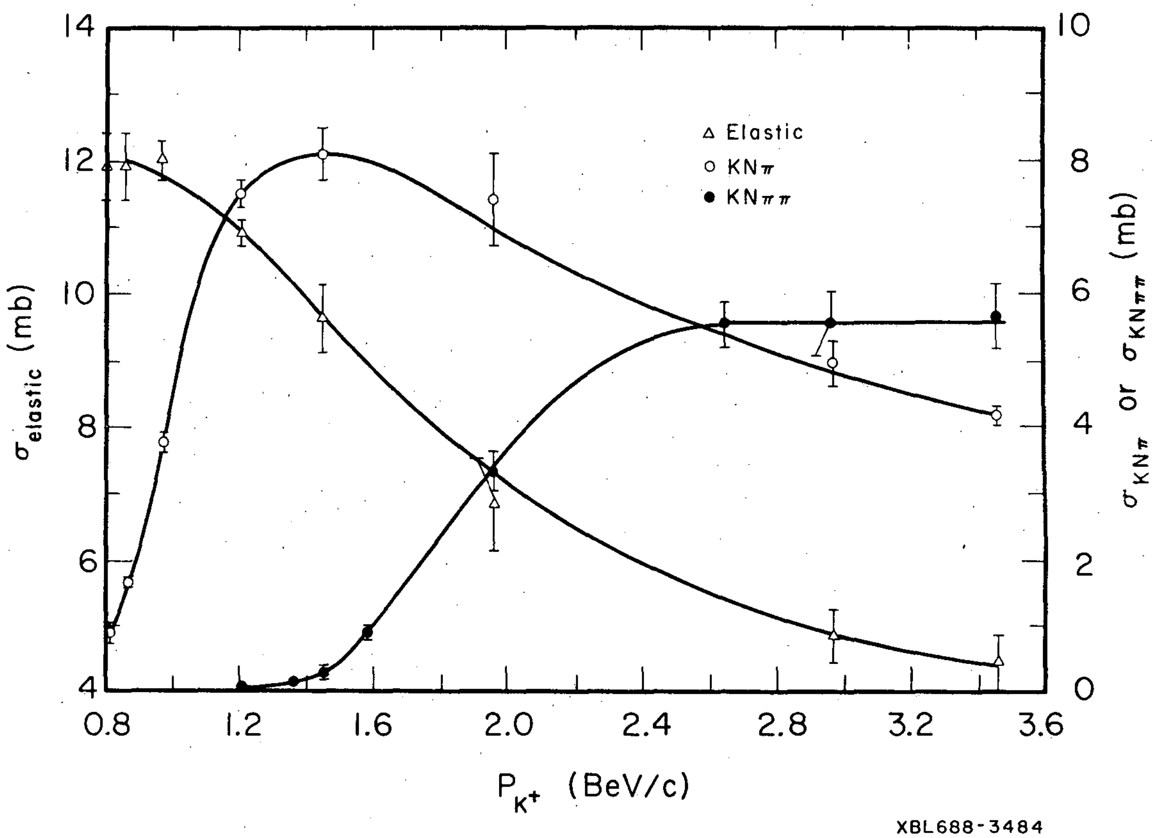

Fig. 2. Elastic, KNπ and KNππ cross sections. The curves are smooth, hand-drawn fits to the points. Note separate scales for elastic and inelastic cross sections.

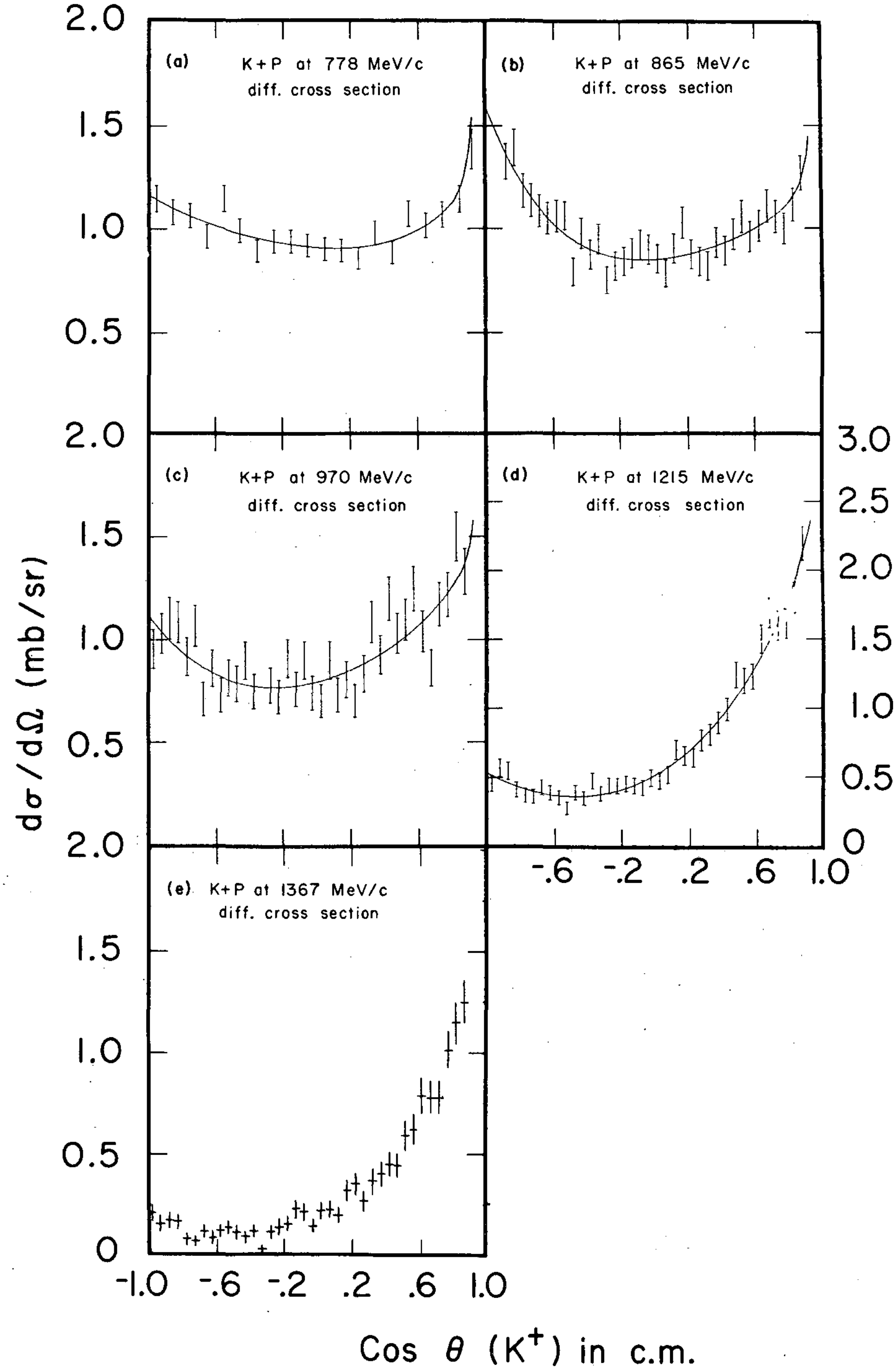

Fig. 3. Elastic differential cross sections at 780, 860, 960, 1200 and 1360 MeV/c. The curves drawn in at all but the highest momentum are the results of the phase shift fits discussed in the text. The curves corresponding to the A_I^- and A_{III}^- solutions are indistinguishable in the above scale.

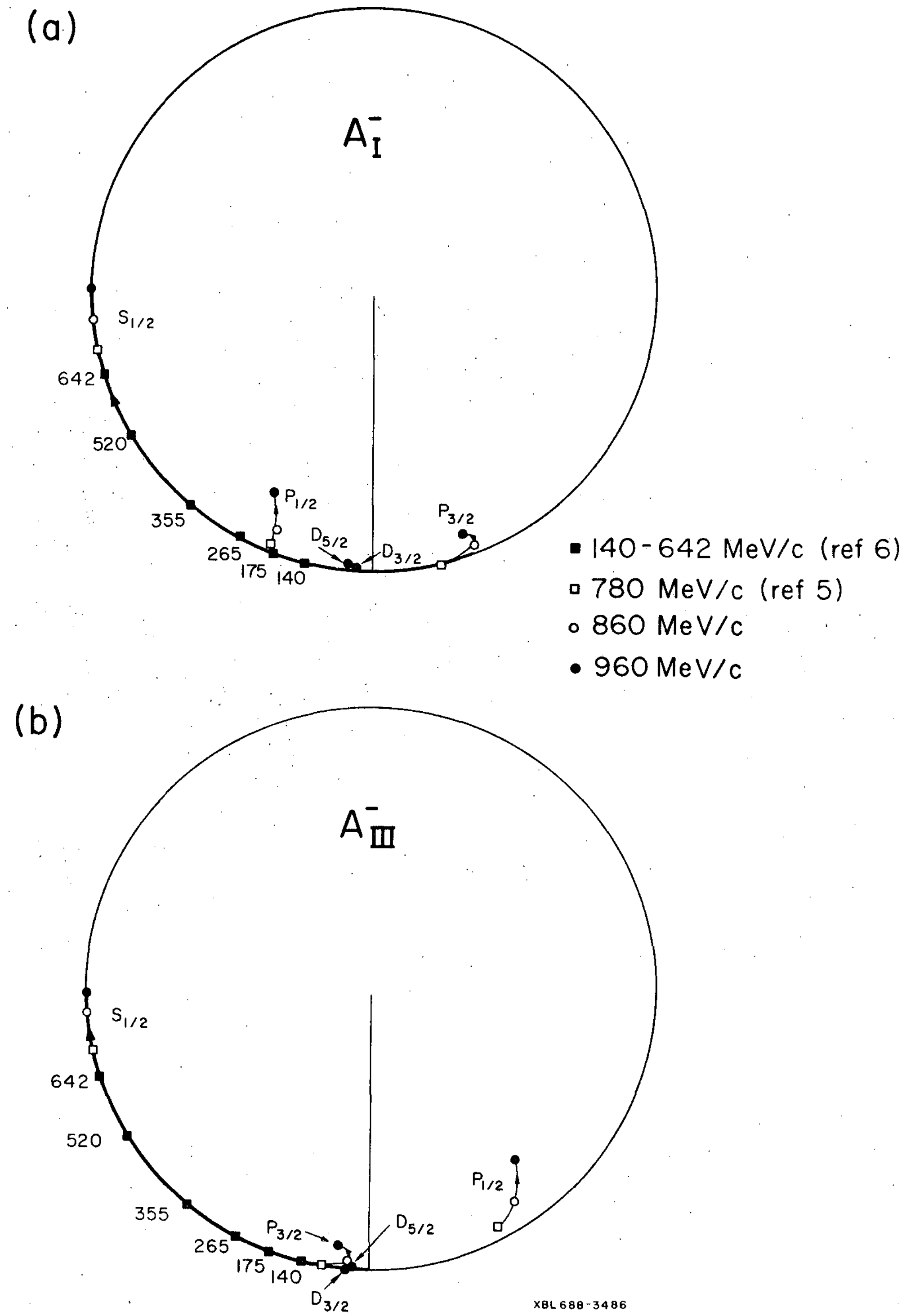

Fig. 4. Argand diagram of the elastic partial wave amplitudes for solutions A_I^- and A_{III}^-. The points at 780 MeV/c represent our fit to the data of Focardi et al.

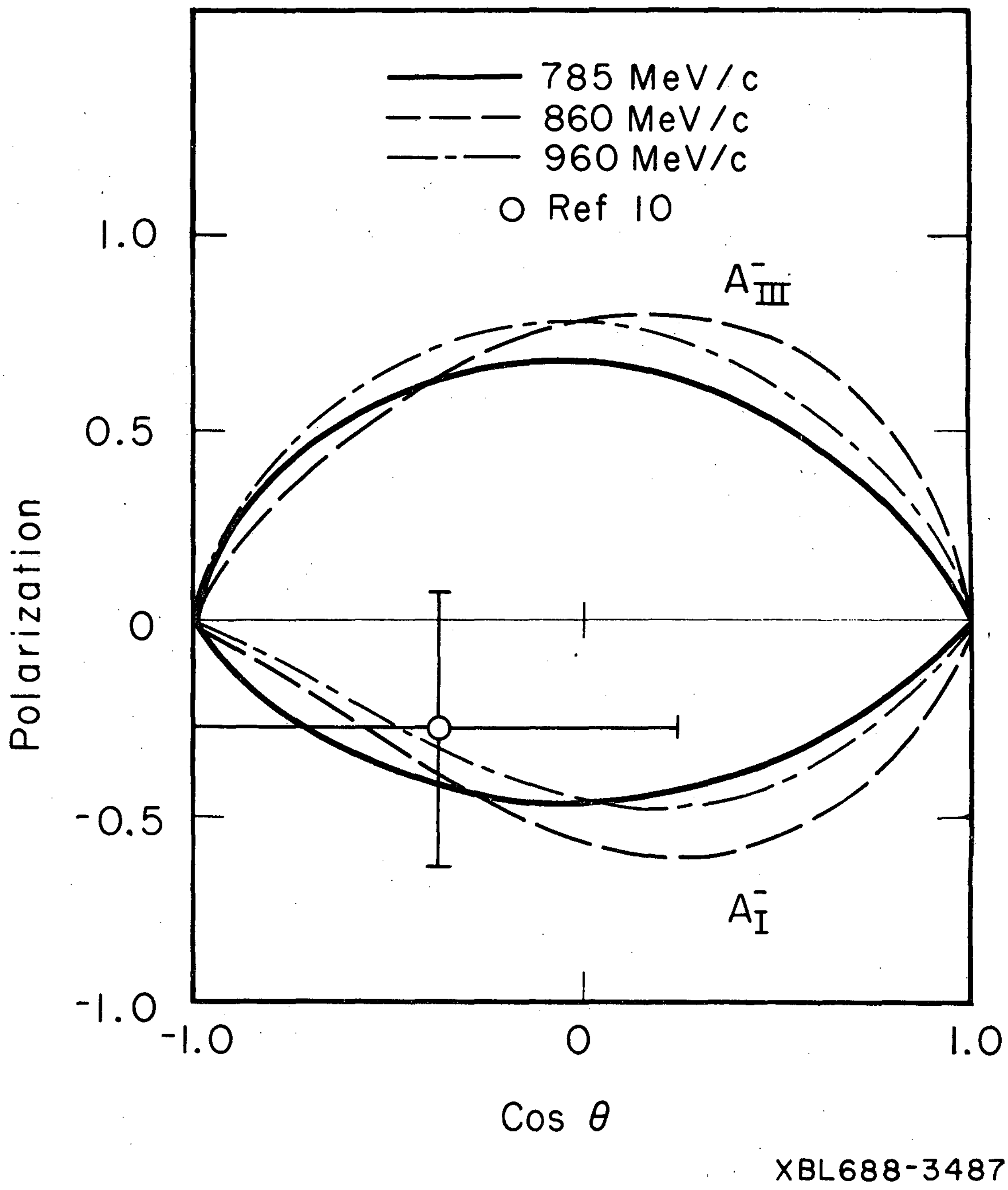

Fig. 5. Predicted polarizations for the A^-_I and A^-_{III} solutions. The experimental point is that of Femino et al.[10]

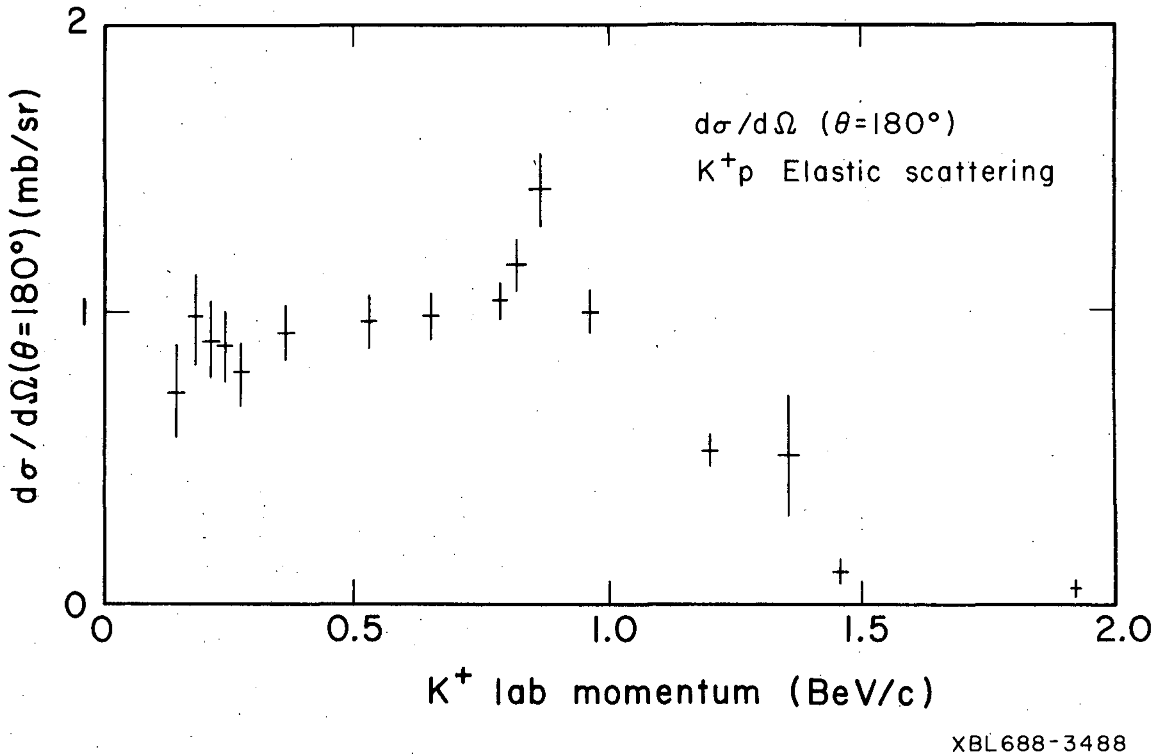

Fig. 6. Variation with K^+ momentum of $d\sigma/d\Omega$ (180°), as given by the backward intercept of a smooth fit to the differential cross section.

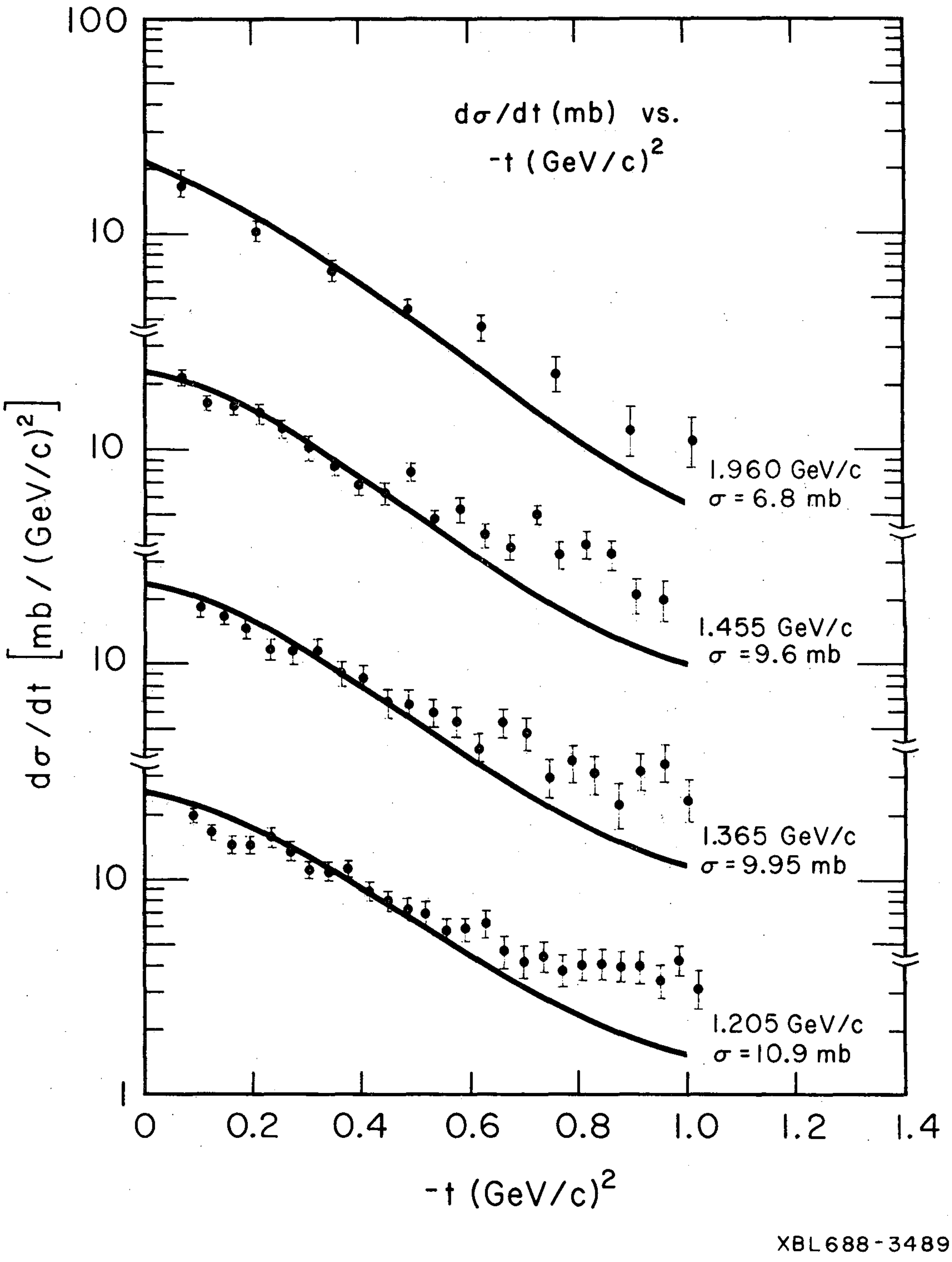

Fig. 7. Semilog plot of $d\sigma/dt$ vs t at 1.2, 1.36, 1.45, and 1.96 BeV/c. The solid curves are from the Regge fit described in the text.

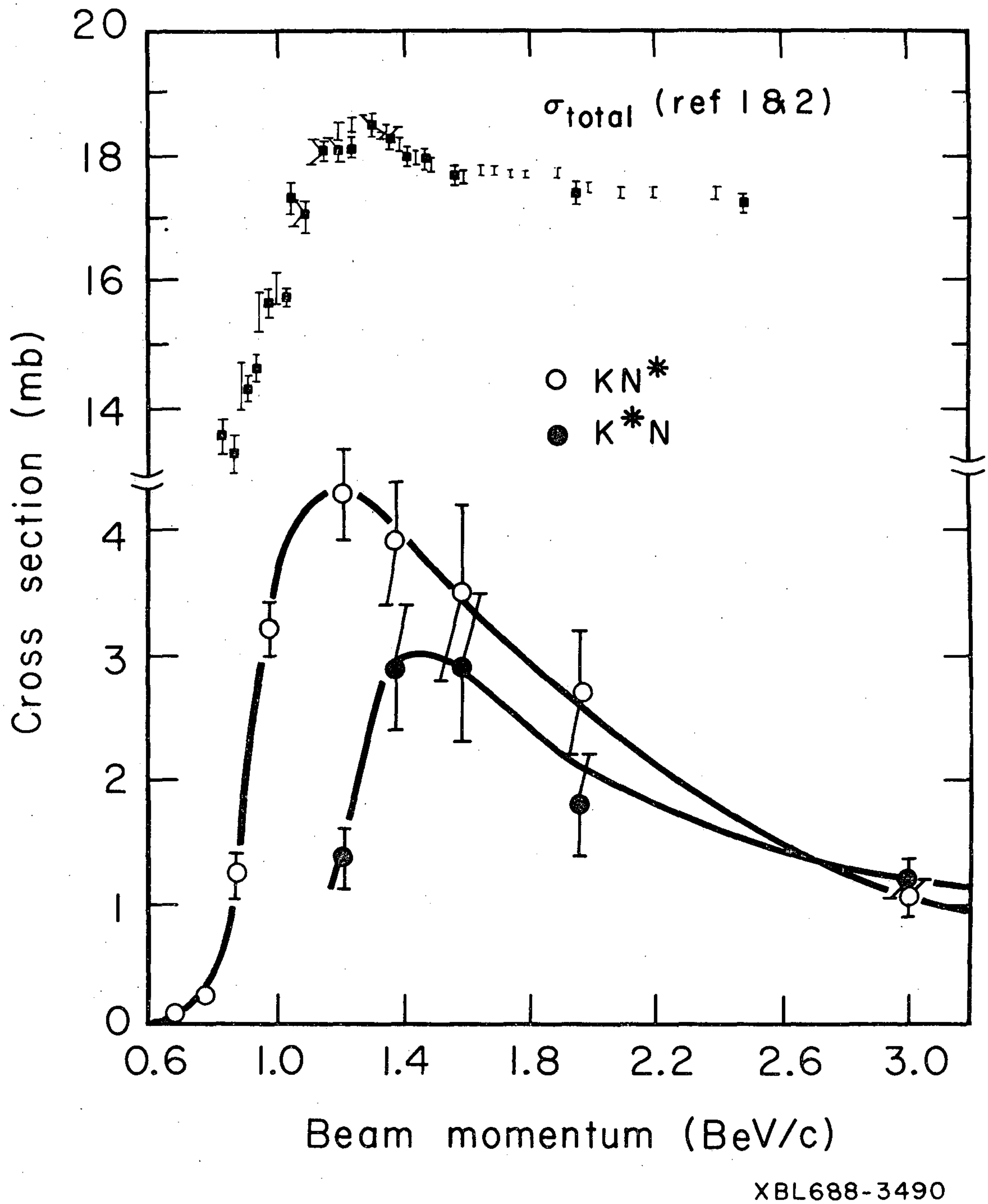

Fig. 8. Cross sections for KN* and NK* production.

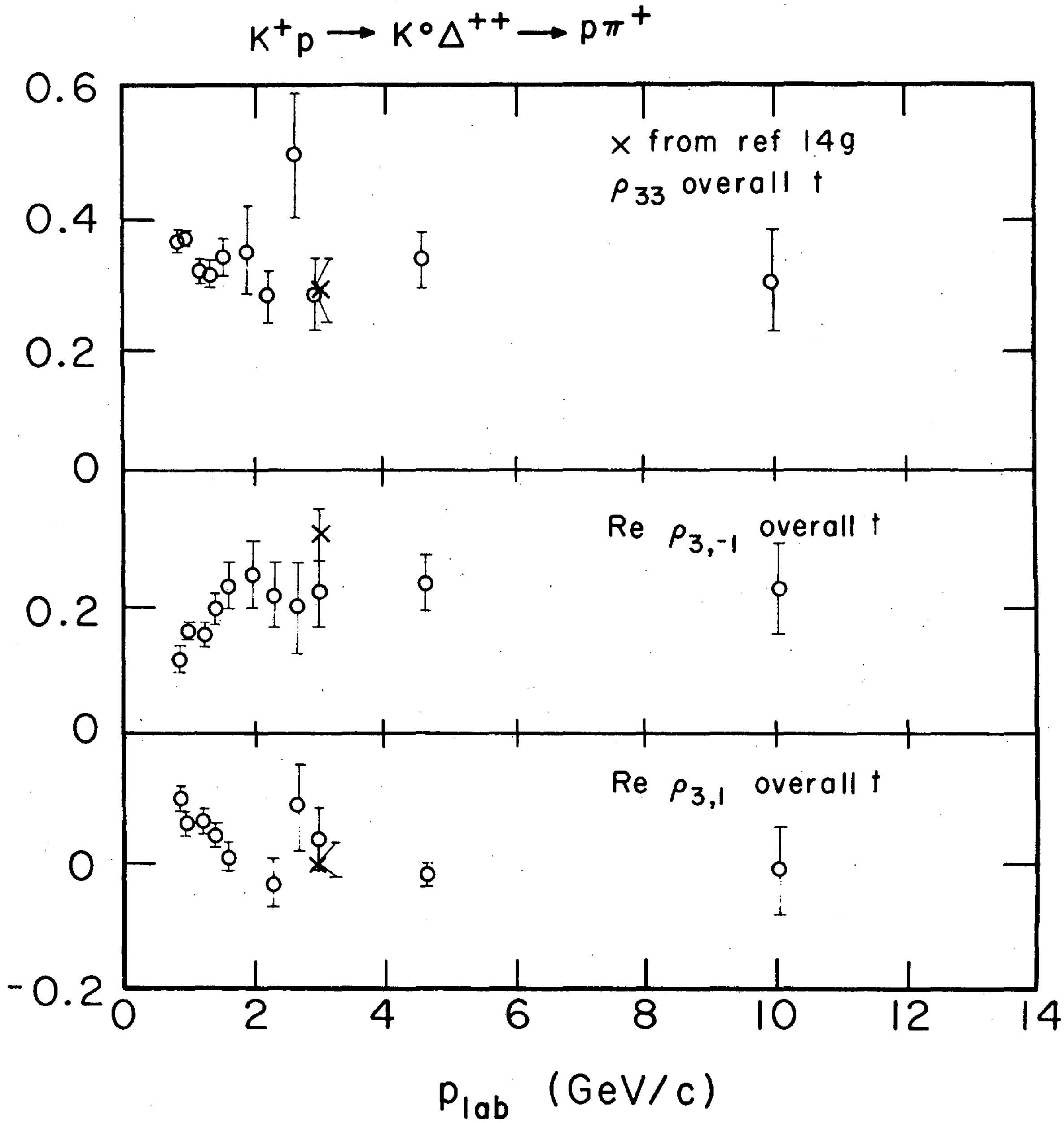

Fig. 9. N^* density matrix elements for various momenta. Compilation by C. Fu.

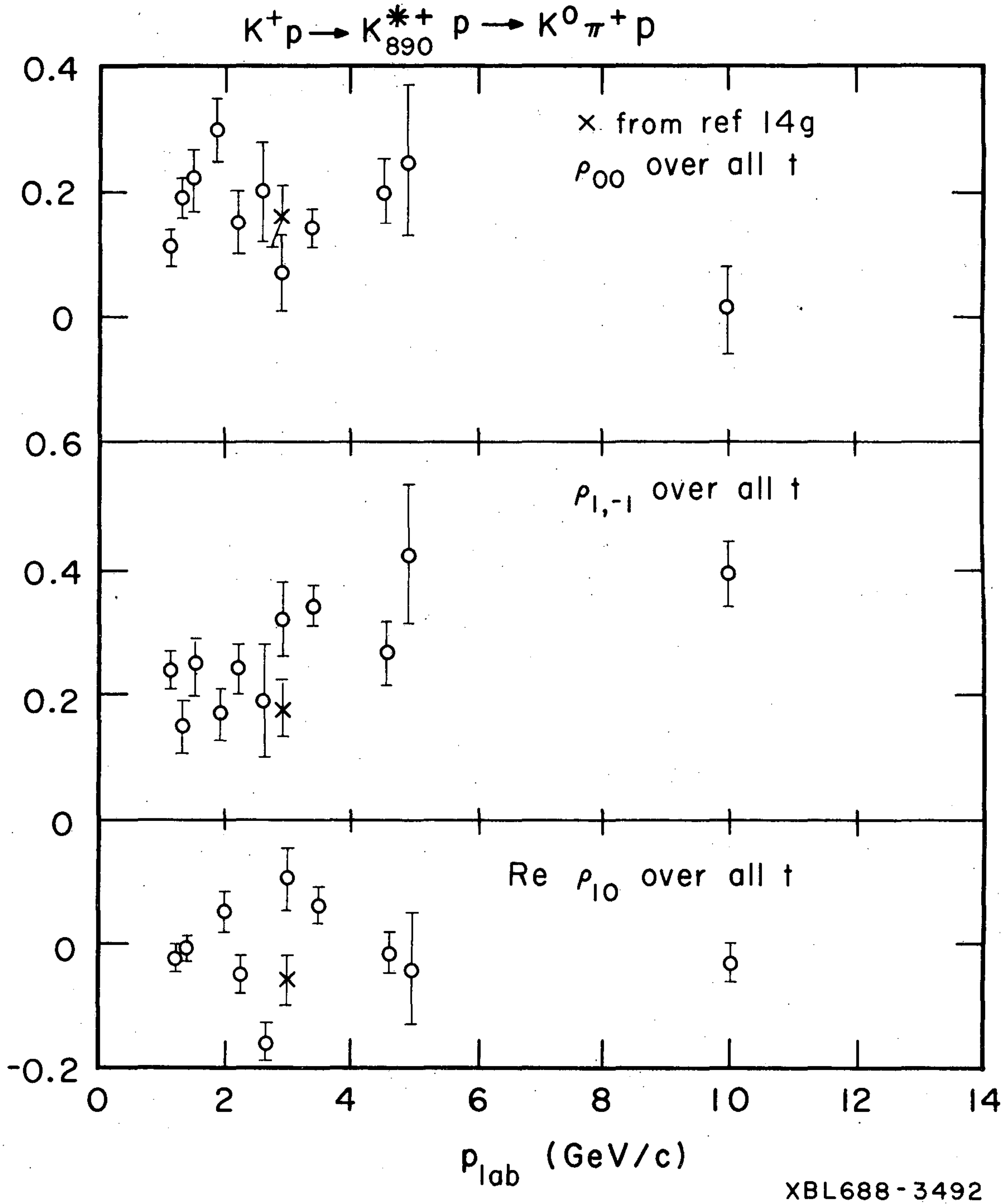

Fig. 10. K^* density matrix elements for various momenta. Compilation by C. Fu.